Dose-Dependent Pulmonary Toxicity of Aerosolized Vitamin E Acetate

Shotaro Matsumoto, Xiaohui Fang, Maret G. Traber, Kirk D. Jones, Charles Langelier, Paula Hayakawa Serpa, Carolyn S. Calfee, Michael A. Matthay, and Jeffrey E. Gotts

Online Data Supplement

Supplementary Methods

Experimental Animals.

Adult 9- to 11- week-old female C57BL/6 mice were purchased from NCI (Frederick, MD, US) and housed under pathogen-free conditions. All experimental procedures were performed under protocols approved by the UCSF Institutional Animal Care and Use Committee. Mice were exposed to aerosol for 1 hour twice daily for between 6 and 15 days, followed by overdose of ketamine, bilateral thoracotomy and exsanguination by right ventricular puncture. Separate animals underwent bronchoalveolar lavage (BAL) by tracheotomy, histology (4% PFA or OCT embedding), or lung harvest for measurement lung water. As in our prior work, samples of whole blood, lung homogenate, and homogenate supernatant were weighed before and after desiccation, such that the volume of blood in the lung could be calculated, permitting measurement of excess extravascular lung water (i.e., pulmonary edema in the interstitial and air spaces above the level in normal mice of the same size).[1] BAL total cell count was measured with a Corning Cell Counter (Cytosmart, Eindhoven, the Netherlands), and cytospin slides of BAL were prepared and stained with Hema 3 solution (Thermo Fisher Scientific, Waltham, MA, US). Differential cell counts were performed at 40x magnification by an observer blinded to condition. BAL protein was measured with the BCA protein assay (Thermo Fisher Scientific), and BAL cytokines were measured by Luminex using a ProcartaPlex multiplex kit from Thermo Fisher Scientific.

Oil red O staining.

Mouse lung was embedded in OCT, and 10 μm frozen sections were collected on charged slides, then processed in propylene glycol and heated Oil Red O stain followed by modified Mayer's hematoxylin (American Mastertech, Lodi, CA, US). AT II cells were fixed on transwell membranes with 4 % PFA, washed with deionized water, and briefly incubated with 60% isopropranol. The cells were then stained with freshly prepared Oil Red O solution (Sigma). Cell nuclei were counterstained with DAPI and brightfield and fluorescence images were merged.

ELISA and multiplex protein analysis

Chemokines in mouse BAL were measured with Luminex using a ProcartaPlex 26 plex kit from Thermo Fisher Scientific. [Eotaxin, granulocyte-macrophage colony stimulating factor (GM-CSF), keratinocyte chemoattractant (KC), interferon (IFN)-γ, interleukin (IL) -1β, IL-10, IL-12p70, IL-13, IL-17A, IL-18, IL-2, IL-22, IL-23, IL-27, IL-4, IL-5, IL-6, IL-9, IFN-inducible protein (IP) -10, monocyte chemotactic protein (MCP) -1, MCP-3, macrophage inflammatory protein (MIP) -1α, MIP-1β, MIP-2, regulated upon activation, normal T-cell expressed and secreted (RANTES), tumor necrosis factor (TNF) - α]. Chemokines in human primary AT II cells culture media were measured with Luminex using a ProcartaPlex multiplex kit from Thermo Fisher Scientific [MIP-1α, stromal cell derived factor (SDF)-1α, C-X-C ligand (CXCL) -10, IL-8, Eotaxin, RANTES, MIP-1β, MCP-1, growth-related gene product (GRO)-α]. Surfactant protein D (SP-D) was measured with a Quantikine ELISA (R&D systems, Minneapolis, MN, US) using an Epoch microplate spectrophotometer (BioTek, Winooski, VT, US).

Human alveolar type II cell isolation and culture

Human alveolar Type II epithelial (AT II) cells were isolated from human lungs declined for transplantation by the Northern California Transplant Donor Network as previously described.[2-4] After cold preservation at 4°C, the right middle lobe was inspected and selected for cell isolation if free of gross consolidation or hemorrhage. The pulmonary vasculature was first flushed antegrade and retrograde with phosphate-buffered saline (PBS) to remove remaining blood from the microcirculation. The distal airspaces were then lavaged 10 times with Ca^{2+},Mg^{2+}-free PBS solution (37°C) containing 0.5 mM EGTA and 0.5 mM EDTA. Elastase, 13 units/ml in Ca^{2+},Mg^{2+}-free Hanks' balanced salt solution, was instilled into the distal airspaces by segmental bronchial intubation. The lobe was then digested at 37 °C for 45–60 min. After digestion, the lobe was further minced in the presence of fetal bovine serum (FBS) and DNase (500 μg/ml). The cell-rich fraction was filtered sequentially through multiple layers of sterile gauze and 100- and 20-μm nylon meshes (Spectra/Mesh, Thermo Fisher Scientific). The filtrate was further layered onto a discontinuous Percoll (Sigma) density gradient of 1.04 and 1.09 g/ml solution and centrifuged at 400 × g for 20 min. The interface containing both AT II cells and alveolar macrophages was collected and further centrifuged at 800 rpm for 10 min, and the cell pellet was washed and resuspended in Ca^{2+},Mg^{2+}-free PBS containing 5% FBS. The cells were incubated with magnetic beads coated with anti-CD 14 antibodies (Dynabeads® CD14, Invitrogen, Carlsbad, CA, US) at 4°C for 40 min, and the majority of the macrophages were then selectively depleted with a Dynal magnet (Dynal Biotech, Oslo, Norway). The cell suspension was further incubated on Petri dishes coated with human IgG antibodies (Sigma) for 4h at 37°C to remove the remaining macrophages. The unattached

remaining cells consisted of the ATII cells and were seeded at a density of 1×10^6 cells/well on collagen I-coated Transwell plates with a pore size of 0.4 μm and a surface area of 0.33 cm^2 (Corning, Sigma). The cells were cultured in a 37°C and 5% CO2 incubator in DMEM high glucose 50%, F-12 50% mix medium containing 10% FBS and antibiotics (penicillin, streptomycin, gentamicin, and amphotericin) for 7 days until they are fully confluent forming a monolayer and tight junctions, tested with visual inspection as described previously[2].

TUNEL staining

AT II cells grown on Transwell membranes were fixed in 4% PFA and stained with TUNEL Assay Kit - BrdU-Red (Abcam, Burlingame, CA, US). Briefly, the cells were first stained with DNA Labeling Solution containing Br-dUTP, then incubated with Anti-BrdU-Red antibody. Transwell membranes were excised and mounted with Prolong Gold antifade reagent with DAPI. Apoptotic AT II cells were imaged and counted using a LEICA SP8 laser scanning confocal microscope (Wetzlar, Germany).

Measurement of α-tocopherol and α-tocopheryl acetate

AT II cells on Transwell membranes (5-7.5 $x10^5$ cells/membrane) were scraped and centrifuged, and cell pellets were flash frozen at -80 C. Lipids were extracted from cells using a one phase solvent system (300 μL, 25:10:65 v/v/methylene chloride: isopropanol: methanol, with 50 μg/mL butylated hydroxytoluene), sonication for 10 sec, followed by incubation at –20°C for 30 minutes and centrifugation at 4°C at 15,000 × g for 10 min.[5] An aliquot (96 μL) of the supernatant was transferred to a mass spectrometry vial, containing internal standards 2 μL hexadeuterium-labeled α-tocopheryl acetate (gift from Dr Dan Liebler, Vanderbilt University) and 2 μL Splash®

Lipidomix® Mass Spec Standards (Avanti Polar Lipids, Alabaster, AL, US)]. Samples were mixed and kept at -80°C until UPLC-MS/MS analysis, as described.[6] The α-tocopheryl acetate was identified using PeakView software (Sciex, Framingham MA, US) and integration was performed using MultiQuant software (Sciex). External standards of α-tocopherol and α-tocopheryl acetate for quantification were purchased from Sigma. Cholesterol and phosphatidyl choline were identified by the software and quantitated by comparison to their internal standard quantities in the Splash mixture.

RNA-Sequencing

AT II cells on Transwell membranes were lysed with RLT Plus buffer, and RNA was extracted with RNeasy Plus Micro kit (Qiagen, Germantown, MD, US). RNA concentrations were measured with a Denovix DS-11FX spectrophotometer/fluorometer. RNA-Seq libraries were built with the NEBNext Ultra II kit (New England Biolabs, Ipswich, MA, US) and paired end sequencing was performed on an Illumina NextSeq instrument (Illumina, San Diego, CA, US). Gene counts were generated using STAR and human genome build 38 (GRCh38) according to previously described methods.[7] Genes present in <30% of samples across an experimental dataset of n=8 samples were excluded from the analysis. The DESeq 2 package[8] in the R computational environment was used for normalization and differential expression analysis. Gene set enrichment analysis was carried out on genes differentially expressed with a false discovery rate <0.1 using WebGestalt ORA[9] and the KEGG functional database. Pathways significantly enriched at a false discovery rate (FDR) <0.1 were identified using a Benjamini-Hochberg multiple test correction.

Figure E1. Vaping Device Schematic. VEA was aerosolized by an atomizer designed for vaping THC oils. A Gram Universal Vaping Machine controls a syringe pump, a 3-way valve, and provides adjustable power output to the atomizer, enabling precise control over aerosol generation (see Supplementary Methods). Aerosol was injected into an approximately 25 L exposure chamber for whole body mouse exposure; for cell culture exposure, a dedicated chamber was placed inside a cell culture incubator that controlled ambient temperature, humidity, and CO_2 within a narrow range. To create steady state conditions, air was removed from the chamber at 2.0 liter/minute and fresh aerosol was injected during the entire exposure, with the volume inflow balance derived from the room (for mice) or the cell culture incubator, providing a source of fresh air.

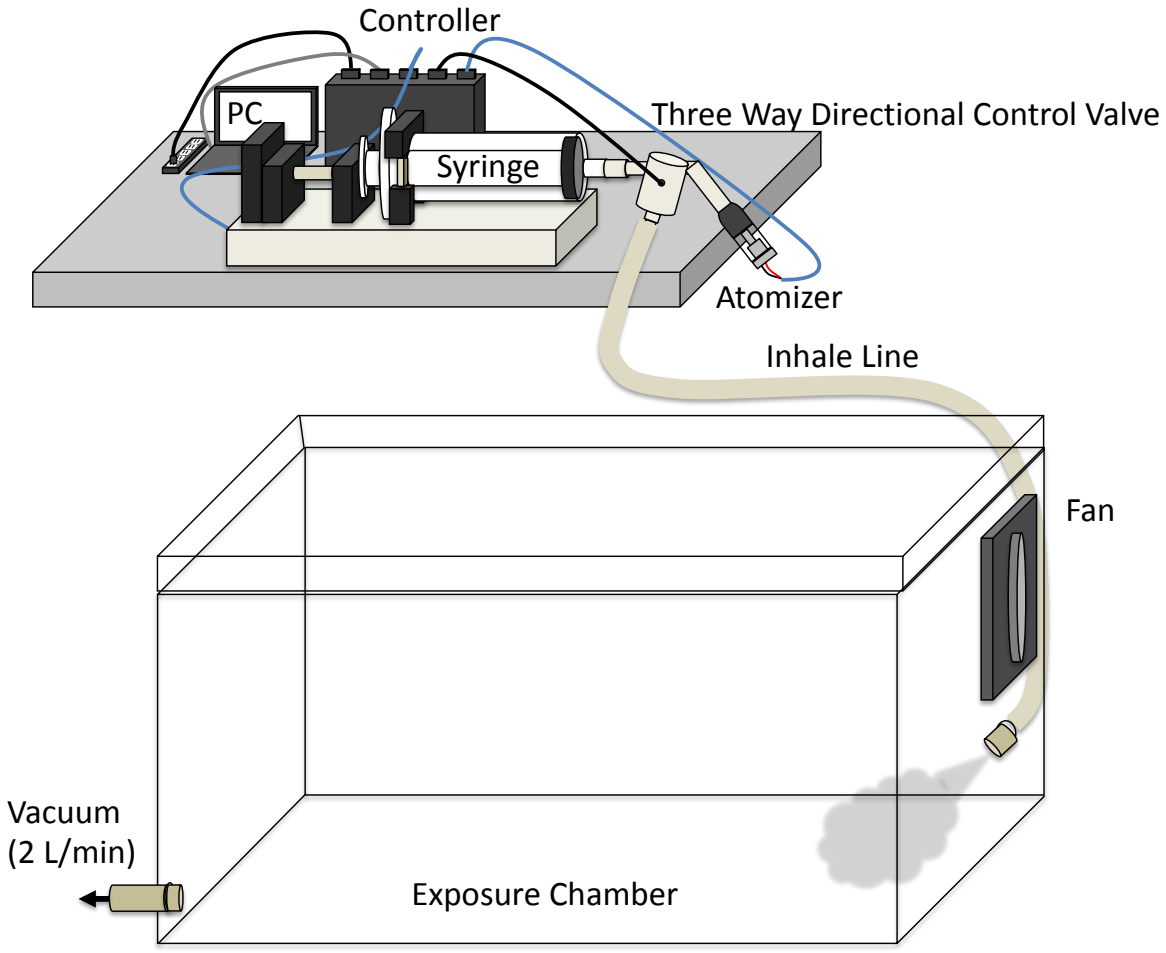

Figure E2. VG/PG aerosolized by ceramic coils does not cause significant lung injury. Mice were exposed to VEA or a 1:1 mixture of VG and PG aerosolized by a ceramic coil using identical power and puffing conditions as in **Figure 1**. Excess lung water (left panel) and BAL protein (right panel) were significantly increased by VEA but not VG/PG. Statistical differences between groups were calculated by Kruskal Wallis followed by Dunn's MCT. *$P < 0.05$.

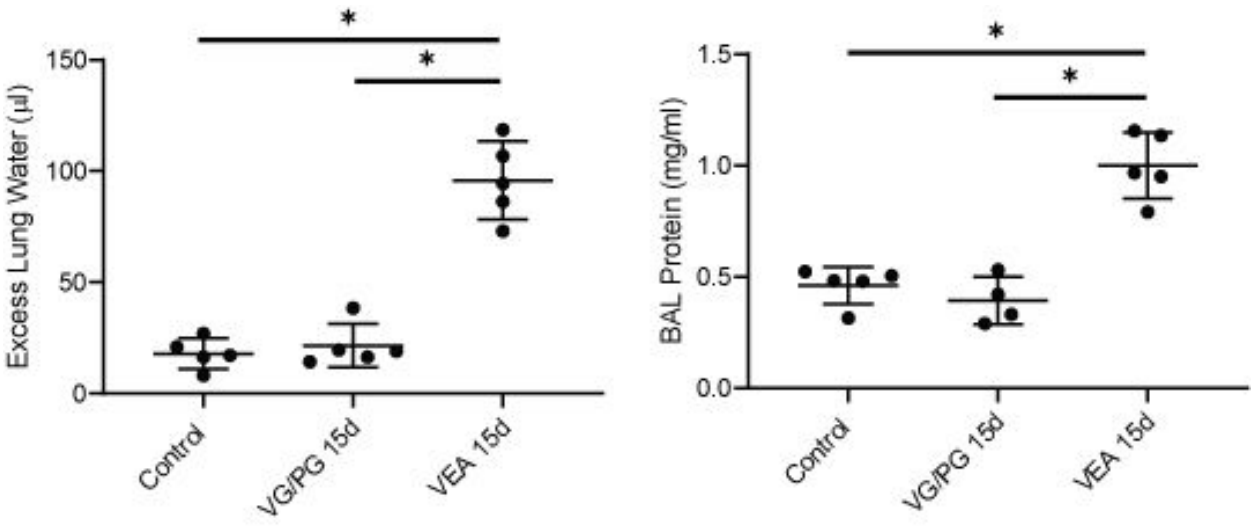

Figure E3. Oil Red O staining of BAL cytopsin after 6 days of VEA exposure reveals large oil-filled macrophages. BAL recovered from a mouse exposed to VEA for 6 days was prepared on a cytospin slide and stained with Oil Red O. Some but not all alveolar macrophages demonstrated large oil-containing vacuoles.

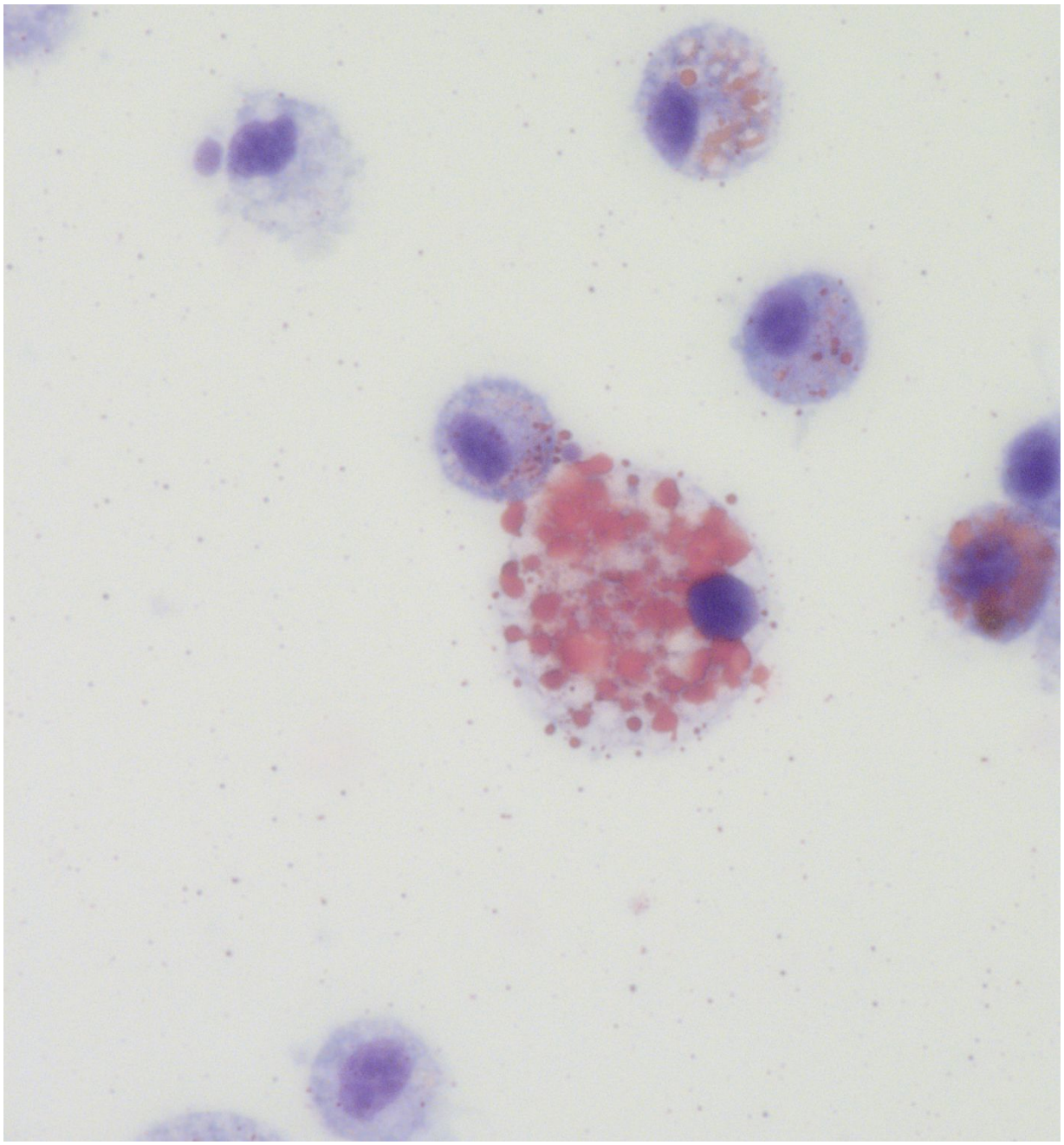

Figure E4. LDH release from VEA-exposed AT II cells is accompanied by positive TUNEL labeling. AT II cells on transwells underwent TUNEL labeling (see Supplementary Methods). Increased TUNEL+ AT II cells (arrow) were observed following VEA exposure in comparison to unexposed cells. The percentage of TUNEL+ cells (TUNEL+/DAPI+) was 0.5% for control and 1.3% for VEA.

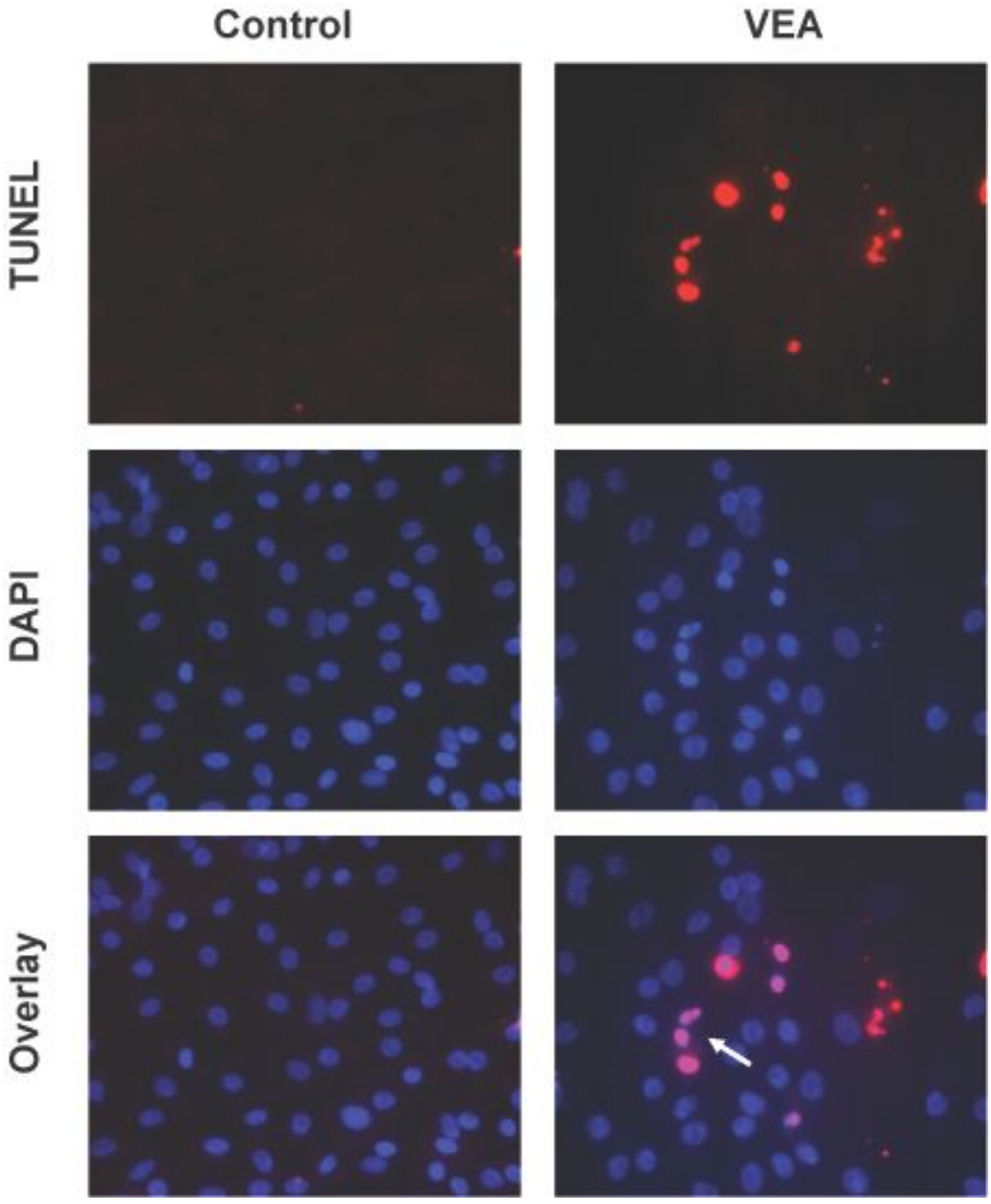

Figure E5. Replication of dose-dependent toxicity of aerosolized VEA in ATII cells. ATII cells were harvested and grown to confluence and air-liquid interface from a separate non-smoking donor. Statistical differences between groups were calculated by ANOVA followed by Tukey's MCT. *P < 0.05, ***P <0.001.

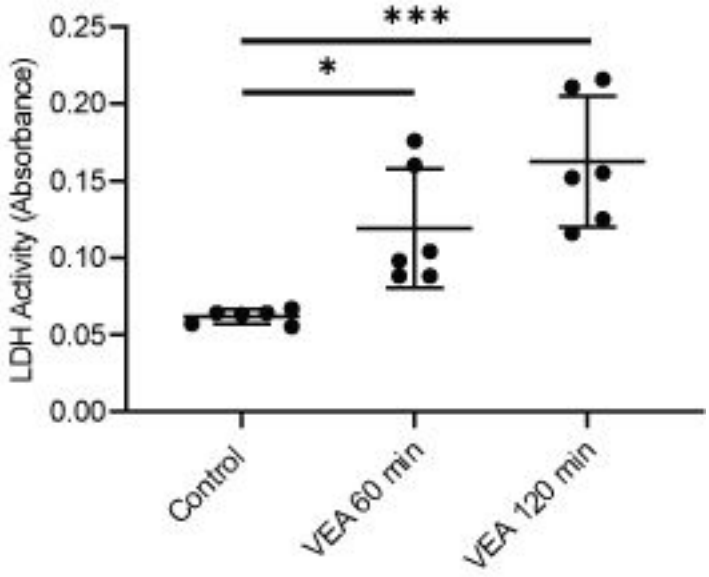

Figure E6. VEA causes dose-dependent inflammatory chemokine release from human AT II cells. AT cells on transwells were exposed to between 20 minutes and 120 minutes of VEA aerosol daily for 3 consecutive days. Luminex analysis of inflammatory chemokines in the media (see Supplementary Methods) revealed dose-dependent increases. Statistical difference between groups were calculated with one-way ANOVA followed by Tukey's MCT (SDF-1α, CXCL10, Eotaxin, MIP-1β) or Kruskal-Wallis followed by Dunn's MCT (MIP-1α, IL-8, RANTES, MCP-1, GRO-α). *p<0.05, **p<0.01, ***p<0.001

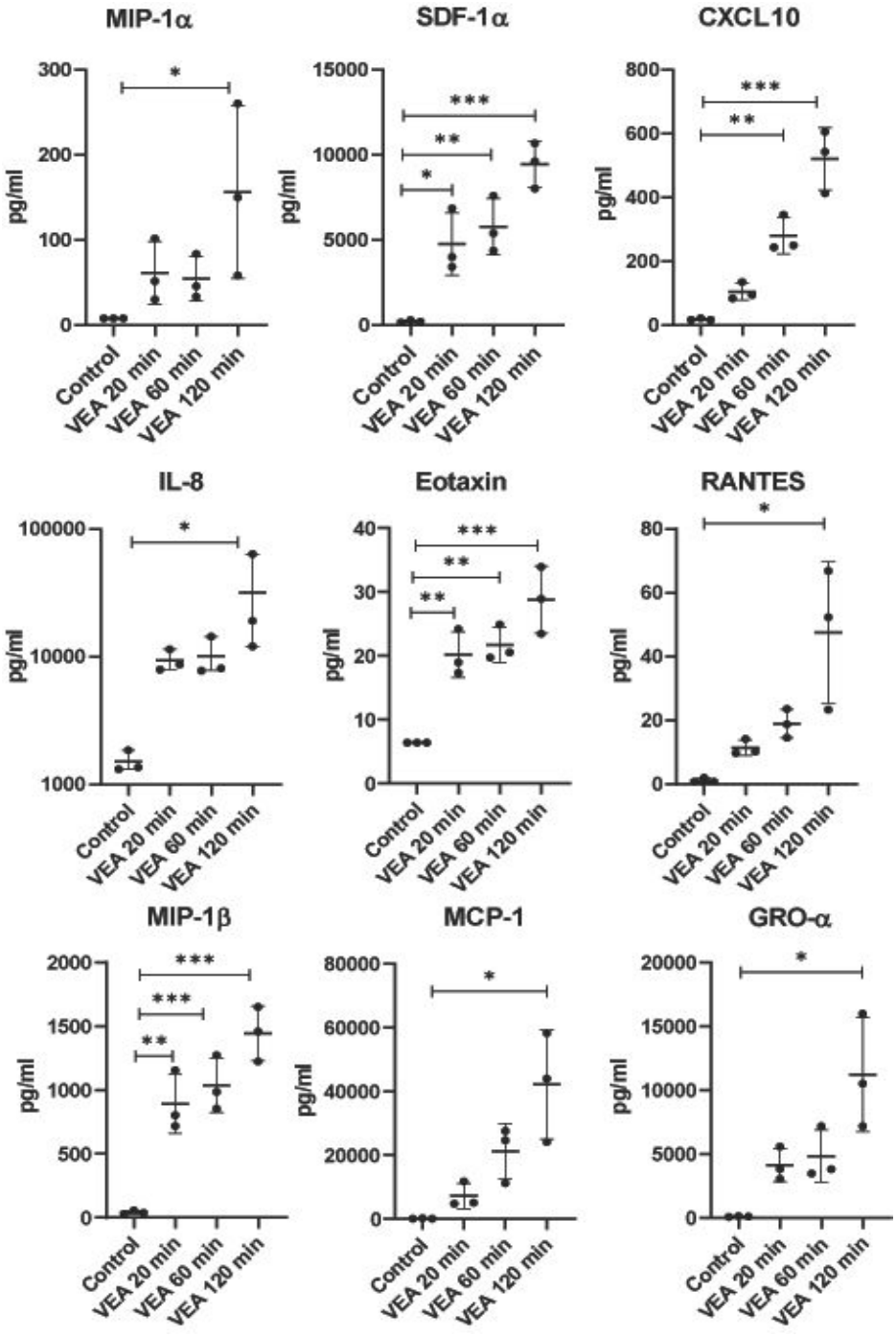

Figure E7. Principal component analysis plot of gene expression colored by Control versus VEA-exposed cells.

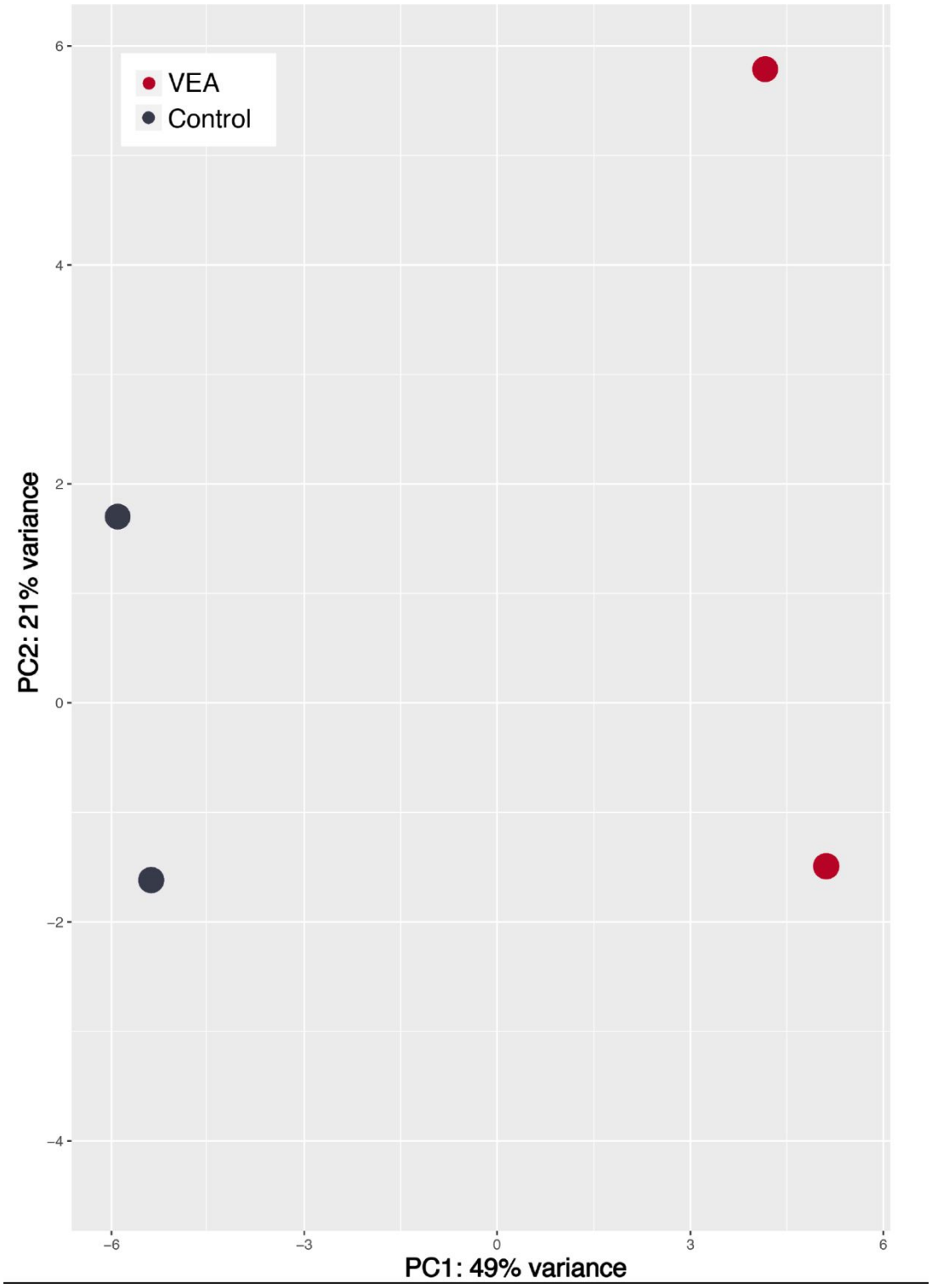

Figure E8. Volcano plot of enriched pathways in RNA-seq following VEA aerosol exposure.

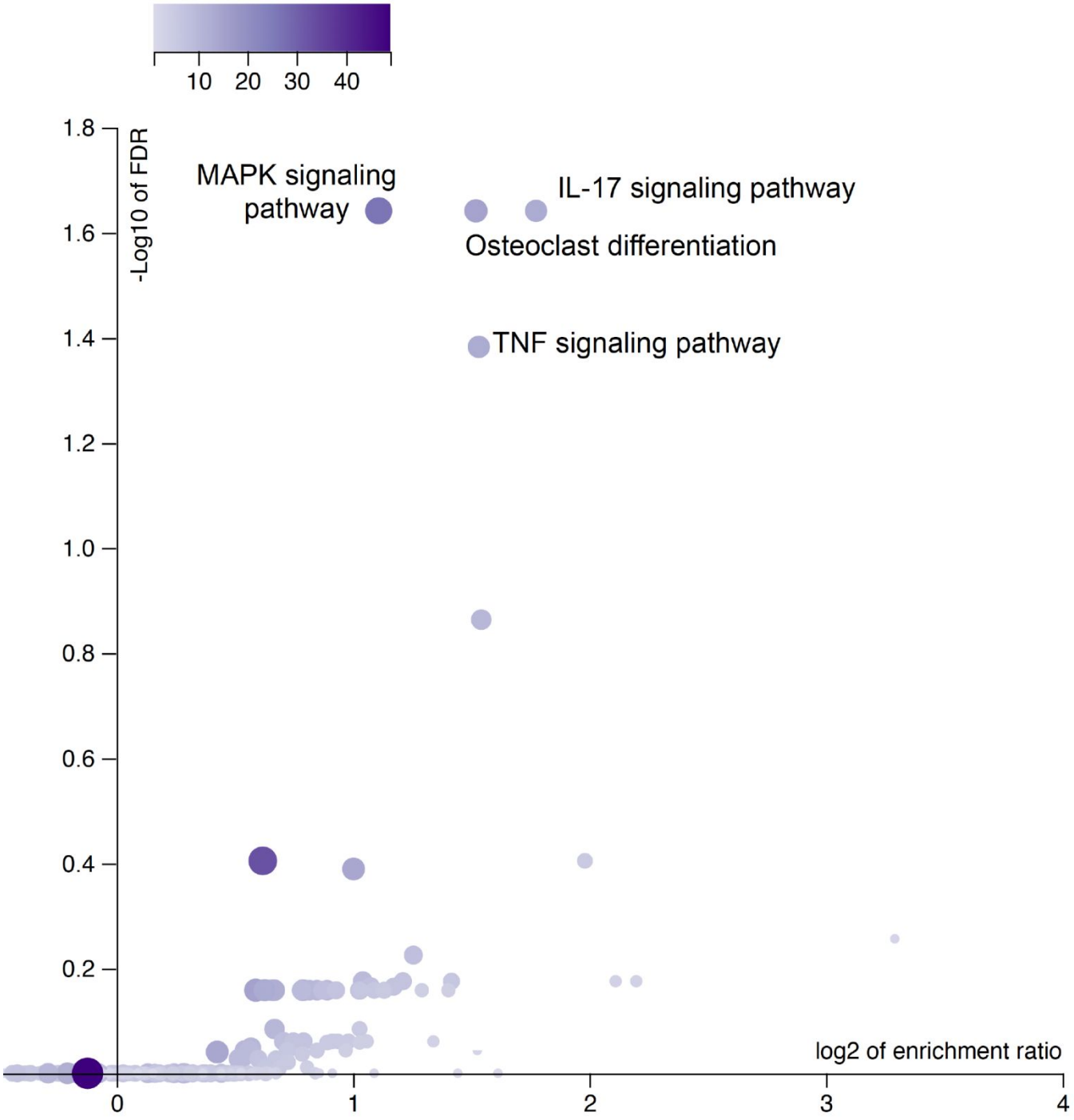

Table E1. Genes in enriched pathways following VEA aerosol exposure.

	Human Symbol	Gene ID
IL-17 signaling	PTGS2	prostaglandin-endoperoxide synthase 2
	IL17RE	interleukin 17 receptor E
	MAPK8	mitogen-activated protein kinase 8
	MUC5AC	mucin 5AC, oligomeric mucus/gel-forming
	FOSL1	FOS like 1, AP-1 transcription factor subunit
	NFKBIA	NFKB inhibitor alpha
	TRAF4	TNF receptor associated factor 4
	CCL2	C-C motif chemokine ligand 2
	JUND	JunD proto-oncogene, AP-1 transcription factor subunit
	FOSB	FosB proto-oncogene, AP-1 transcription factor subunit
MAPK signaling	FOS	Fos proto-oncogene, AP-1 transcription factor subunit
	KITLG	KIT ligand
	JUN	Jun proto-oncogene, AP-1 transcription factor subunit
	EFNA1	ephrin A1
	MAP3K13	mitogen-activated protein kinase kinase kinase 13
	HSPB1	heat shock protein family B
	HSPA1A	heat shock protein family A (Hsp70) member 1A
	DUSP1	dual specificity phosphatase 1
	HSPA8	heat shock protein family A (Hsp70) member 8
	TGFBR2	transforming growth factor beta receptor 2
	IL1R1	interleukin 1 receptor type 1
	RAPGEF2	Rap guanine nucleotide exchange factor 2
	CRKL	CRK like proto-oncogene, adaptor protein
	MAPK8	mitogen-activated protein kinase 8
	DUSP10	dual specificity phosphatase 10
	EPHA2	EPH receptor A2
	ATF4	activating transcription factor 4
	RELB	RELB proto-oncogene, NF-kB subunit
	JUND	JunD proto-oncogene, AP-1 transcription factor subunit
	DUSP7	dual specificity phosphatase 7
	NR4A1	nuclear receptor subfamily 4 group A member 1
	CACNA1D	calcium voltage-gated channel subunit alpha1 D
	DUSP4	dual specificity phosphatase 4
	CACNA1H	calcium voltage-gated channel subunit alpha1 H
	RASGRP3	RAS guanyl releasing protein 3
	KIT	KIT proto-oncogene, receptor tyrosine kinase
Osteoclast differentiation	FOS	Fos proto-oncogene, AP-1 transcription factor subunit
	FCGR2A	Fc fragment of IgG receptor IIa
	SOCS3	suppressor of cytokine signaling 3
	JUN	Jun proto-oncogene, AP-1 transcription factor subunit
	TGFBR2	transforming growth factor beta receptor 2
	IL1R1	interleukin 1 receptor type 1
	MAPK8	mitogen-activated protein kinase 8
	FOSL2	FOS like 2, AP-1 transcription factor subunit
	RELB	RELB proto-oncogene, NF-kB subunit
	JUND	JunD proto-oncogene, AP-1 transcription factor subunit
	NFKBIA	NFKB inhibitor alpha
	PPARG	peroxisome proliferator activated receptor gamma
	FOSB	FosB proto-oncogene, AP-1 transcription factor subunit
	FOSL1	FOS like 1, AP-1 transcription factor subunit
TNF signaling	FOS	Fos proto-oncogene, AP-1 transcription factor subunit
	CXCL2	C-X-C motif chemokine ligand 2
	EDN1	endothelin 1
	SOCS3	suppressor of cytokine signaling 3
	JUN	Jun proto-oncogene, AP-1 transcription factor subunit
	MAPK8	mitogen-activated protein kinase 8
	BCL3	BCL3 transcription coactivator
	JAG1	jagged canonical Notch ligand 1
	ATF4	activating transcription factor 4
	CFLAR	CASP8 and FADD like apoptosis regulator
	NFKBIA	NFKB inhibitor alpha
	PTGS2	prostaglandin-endoperoxide synthase 2
	CCL2	C-C motif chemokine ligand 2

References

E1. Su X, Lee JW, Matthay ZA, et al. Activation of the alpha7 nAChR reduces acid-induced acute lung injury in mice and rats. Am J Respir Cell Mol Biol 2007;37:186–192.

E2. Fang X, Song Y, Hirsch J, et al. Contribution of CFTR to apical-basolateral fluid transport in cultured human alveolar epithelial type II cells. Am J Physiol Lung Cell Mol Physiol 2006;290:L242-249.

E3. Lee JW, Fang X, Dolganov G, et al. Acute lung injury edema fluid decreases net fluid transport across human alveolar epithelial type II cells. J Biol Chem 2007;282:24109–24119.

E4. Fang X, Neyrinck AP, Matthay MA, Lee JW. Allogeneic human mesenchymal stem cells restore epithelial protein permeability in cultured human alveolar type II cells by secretion of angiopoietin-1. J Biol Chem 2010;285:26211–26222.

E5. McDougall MQ, Choi J, Stevens JF, Truong L, Tanguay RL, Traber MG. Lipidomics and H2(18)O labeling techniques reveal increased remodeling of DHA-containing membrane phospholipids associated with abnormal locomotor responses in α-tocopherol deficient zebrafish (danio rerio) embryos. Redox Biol 2016;8:165–74.

E6. Choi J, Leonard SW, Kasper K, et al. Novel function of vitamin E in regulation of zebrafish (Danio rerio) brain lysophospholipids discovered using lipidomics. J Lipid Res 2015;56:1182–1190.

E7. Langelier C, Kalantar KL, Moazed F, et al. Integrating host response and unbiased microbe detection for lower respiratory tract infection diagnosis in critically ill adults. Proc Natl Acad Sci USA 2018;115:E12353–12362.

E8. Love MI, Huber W, Anders S. Moderated estimation of fold change and dispersion for RNA-seq data with DESeq2. Genome Biol 2014;15:550.

E9. Liao Y, Wang J, Jaehnig EJ, Shi Z, Zhang B. WebGestalt 2019: gene set analysis toolkit with revamped UIs and APIs. Nucleic Acids Res 2019;47:W199–205.